

Water adsorption on $O(2 \times 2)/Ru(0001)$: STM experiments and first-principles calculationsPepa Cabrera-Sanfelix,¹ Daniel Sánchez-Portal,² Aitor Mugarza,^{3,4} Tomoko K. Shimizu,^{3,5} Miquel Salmeron,^{3,5} and Andrés Arnau^{2,6}¹*Donostia International Physics Center (DIPC), Manuel de Lardizabal 4, San Sebastián 20018, Spain*²*Unidad de Física de Materiales, Centro Mixto CSIC-UPV, Edificio Kortxa, Avenida de Tolosa 72, San Sebastián 20018, Spain*³*Materials Sciences Division, Lawrence Berkeley National Laboratory, Berkeley, California 94720, USA*⁴*Institut de Ciència de Materials de Barcelona, CSIC, Bellaterra 08193, Spain*⁵*Department of Materials Science and Engineering, University of California Berkeley, California 94709, USA*⁶*Departamento de Física de Materiales, Facultad de Química, UPV/EHU, Apartado 1072, San Sebastián 20080, Spain*

(Received 1 August 2007; published 27 November 2007)

We present a combined theoretical and experimental study of water adsorption on $Ru(0001)$ precovered with 0.25 ML (monolayer) of oxygen forming a (2×2) structure. Several structures were analyzed by means of density functional theory calculations for which scanning tunneling microscope (STM) simulations were performed and compared with experimental data. Up to 0.25 ML, the molecules bind to the exposed Ru atoms of the 2×2 unit cell via the lone pair orbitals. The molecular plane is almost parallel to the surface with its H atoms pointing toward the chemisorbed O atoms of the 2×2 unit cell forming hydrogen bonds. The existence of these additional hydrogen bonds increases the adsorption energy of the water molecule to approximately 616 meV, which is ~ 220 meV more stable than on the clean $Ru(0001)$ surface with a similar configuration. The binding energy shows only a weak dependence on water coverage, with a shallow minimum for a row structure at 0.125 ML. This is consistent with the STM experiments that show a tendency of the molecules to form linear rows at intermediate coverage. Our calculations also suggest the possible formation of water dimers near 0.25 ML.

DOI: [10.1103/PhysRevB.76.205438](https://doi.org/10.1103/PhysRevB.76.205438)

PACS number(s): 68.43.Bc, 68.37.Ef, 68.55.Jk

I. INTRODUCTION

At low coverage, water binds preferentially atop adsorption sites on metal surfaces with its molecular dipole almost parallel to the surface.¹ The increase of water coverage gives rise to the formation of dimers, trimers, hexamers, and finally clusters and honeycomb structures.^{2–6} While these initial water structures on clean metal surfaces are of fundamental interest in wetting, electrochemistry, and chemical reaction studies, it is also very important to understand the adsorption of water on oxides and on oxygen covered metal surfaces. This is because oxygen atoms at the surface might change significantly the binding of water^{4,7,8} due to the possibility of formation of hydrogen bonds with the water molecules.

Indeed, on a $Rh(111)$ surface with a dense oxygen overlayer forming a (1×1) structure,⁹ it has been proposed that the first layer of water binds via formation of H bonds with the surface O atoms. In a recent x-ray study¹⁰ of water adsorption on $O(2 \times 2)/Ni(111)$, two different water structures have been identified. On $Ru(0001)$, a transition from covalent bonding to the Ru atoms to hydrogen bonding to the O atoms on the $O(1 \times 1)/Ru(0001)$ surface has been proposed.¹¹ Recently, in a combined x-ray photoemission spectroscopy and thermal desorption spectroscopy study of water on $Ru(0001)$ as a function of O coverage, a transition from thermally activated dissociative adsorption for O coverage $\theta < 0.25$ ML (monolayer) to nondissociative adsorption for $\theta > 0.25$ ML has been observed, strongly suggesting a related change in the adsorption configuration of water.¹²

In this work, we present a combined theoretical and experimental study of water adsorption on the $O(2$

$\times 2)/Ru(0001)$ surface structure. Different adsorption geometries are found and discussed in detail. Simulated scanning tunneling microscope (STM) images from these structures are then compared with the experimental images. We find that water molecules adsorb covalently on Ru-top sites and form additional hydrogen bonds with the O atoms of the $O(2 \times 2)/Ru(0001)$ surface. The additional H bonding increases the adsorption energy appreciably with respect to that on the clean substrate. The calculated adsorption energies show a weak dependence on water coverage, with a shallow minimum for a row structure at 0.125 ML, consistent with the experimental STM images that show a tendency of the molecules to form rows at intermediate coverage and a stable water (2×2) superstructure near 0.25 ML. Our calculations also predict that structures formed by monomers and dimers at high and intermediate coverages are almost energetically degenerate.

II. THEORETICAL METHOD

Our density functional theory calculations were performed using the Vienna package (VASP),^{13–15} within the Perdew-Wang 1991 (PW91) version of the general gradient approximation.¹⁶ The projector augmented wave^{17,18} method was used to describe the interaction of electrons with Ru, O, and H atoms.

A symmetric slab of seven Ru layers and the same amount of vacuum was used to represent the $Ru(0001)$ surface. The oxygen and water adsorbates are placed on each surface of the symmetric slab. A plane-wave cutoff of 400 eV and a $6 \times 6 \times 1$ k -point sampling was used for the smallest cell, corresponding to a 2×2 unit cell of the $Ru(0001)$ clean surface.

For the larger 4×4 unit cell used to represent lower water coverages, the k -point sampling was reduced to $3 \times 3 \times 1$. Previous to water deposition, oxygen atoms are adsorbed on hcp sites at 1.17 \AA above the Ru topmost layer.^{19,20} This geometry was optimized by allowing relaxation of all degrees of freedom of the two outermost Ru layers and the O atoms until residual forces were smaller than 0.03 eV/\AA . After the addition of water, all adsorbates, together with top and bottom Ru layers, were allowed to relax in all directions of space during the structural optimization. This procedure was considered to be accurate enough since the adsorption energy of water at 0.25 ML coverage only changed by 10 meV when all atoms, except those Ru atoms in the middle of the slab, were allowed to relax.

The adsorption energy of the water molecule E_{ads} is calculated from

$$E_{ads} = -(E_{\text{H}_2\text{O}/\text{O}(2 \times 2)/\text{Ru}(0001)} - E_{\text{O}(2 \times 2)/\text{Ru}(0001)} - E_{\text{H}_2\text{O}}^{isol}), \quad (1)$$

where $E_{\text{H}_2\text{O}/\text{O}(2 \times 2)/\text{Ru}(0001)}$ is the energy of the optimized system, $E_{\text{O}(2 \times 2)/\text{Ru}(0001)}$ corresponds to the energy of the relaxed $\text{O}(2 \times 2)/\text{Ru}(0001)$ surface calculated in the same conditions (k points, cutoff and unit cell), and $E_{\text{H}_2\text{O}}^{isol}$ is the energy of the relaxed water monomer isolated in vacuum with the same 4×4 supercell. Taken into account the different sources of uncertainty, we estimate an error bar for the calculated adsorption energies of $\sim 10 \text{ meV}$.

The STM simulations were performed using the Tersoff-Hamann^{21,22} approximation.

III. EXPERIMENTAL METHOD

The experiments were performed using a homebuilt low temperature scanning tunneling microscope (STM).²³ The base pressure in the STM chamber was $< 2 \times 10^{-11}$ Torr, and all data were collected at 6 K using electrochemically etched W tips. A single crystal Ru(0001) sample was initially cleaned by a few cycles of Ar ion sputtering and annealing to 1500 K. In order to remove carbon impurities, cycles of heating and cooling from 750 to 1500 K were performed in an O_2 pressure of 1×10^{-7} Torr. The sample was finally flash annealed to 1650 K in order to remove the excess O. After cleaning the sample, O_2 gas was leaked into the chamber at a pressure of 1×10^{-8} Torr for 60 s [0.6 L ($1 \text{ L} = 10^{-6} \text{ Torr s}$)]. This produced a (2×2) -O superstructure, as determined by STM before dosing water.

Water was dosed through a leak valve with a dosing tube pointing at the sample. The source was Milli-Q water in a glass tube further purified by repeated cycles of freezing, pumping, and thawing prior to the introduction into the chamber. In the STM body, the sample was heated when necessary with a resistor mounted near the sample plate, and the temperature controlled with a Si diode mounted between the resistor and the sample.

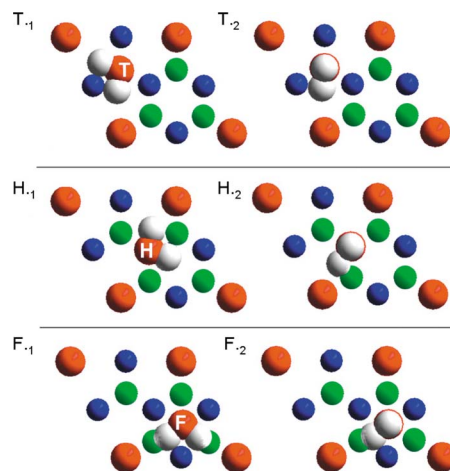


FIG. 1. (Color online) Schematic drawing of the six initial configurations of water adsorbed on the unit cell of $\text{O}(2 \times 2)/\text{Ru}(0001)$. T, H, and F indicate top, hcp, and fcc adsorption sites, respectively. The numbers 1 and 2 correspond molecular plane orientations that are nearly parallel vertical (H upward) with respect to the surface, respectively. The large red circles represent the substrate oxygen atoms preadsorbed on hcp sites; green circles represent the Ru atoms in the topmost layer (top sites), and blue circles Ru atoms on the second layer (hcp sites).

IV. RESULTS AND DISCUSSION

A. Calculation of the optimal adsorption geometry

To obtain the most stable water adsorption configuration, structural optimizations were carried out starting with the water molecule placed 2 \AA above each of the high symmetry sites of the 2×2 unit cell of the relaxed $\text{O}(2 \times 2)/\text{Ru}(0001)$ surface, Ru top (T), fcc hollow (F), and hcp hollow (H), as shown in Fig. 1. The molecule was initially oriented with its dipole parallel to the substrate or with one hydrogen pointing upward from the surface. All six initial states are shown in Fig. 1. After relaxation, only configuration T_{-1} maintains its initial adsorption site and orientation, with a slight upward displacement of the molecule of 0.37 \AA from its initial height. Water configuration T_{-2} reoriented parallel to the surface after relaxation, ending up with an orientation and adsorption height similar to T_{-1} . The same final configuration was obtained when starting with the configurations shown in H_{-1} and H_{-2} , i.e., the molecules moved spontaneously along the surface to the adjacent top site, keeping the dipole also parallel to the surface. Hence, we can conclude that the “top-site and/or parallel-oriented” configuration, with a distance of 2.37 \AA between the Ru atom and the O atom, is the optimum one. The adsorbed water molecule forms extended hydrogen bonds of 2.38 \AA with the surface oxygen atoms [see Fig. 2(b)]. The adsorption energy for this optimal structure is $E_{ads} = 590 \text{ meV}$ at the coverage of 0.25 ML. The structures F_{-1} and F_{-2} in Fig. 1, where the water molecules were placed on an fcc site, move up to $\sim 3.5 \text{ \AA}$ above the Ru topmost layer during relaxation while keeping the same adsorption site. However, the molecule has negligible adsorption energy on these fcc configurations. Ru-top site and hydrogen bonding between water molecules and

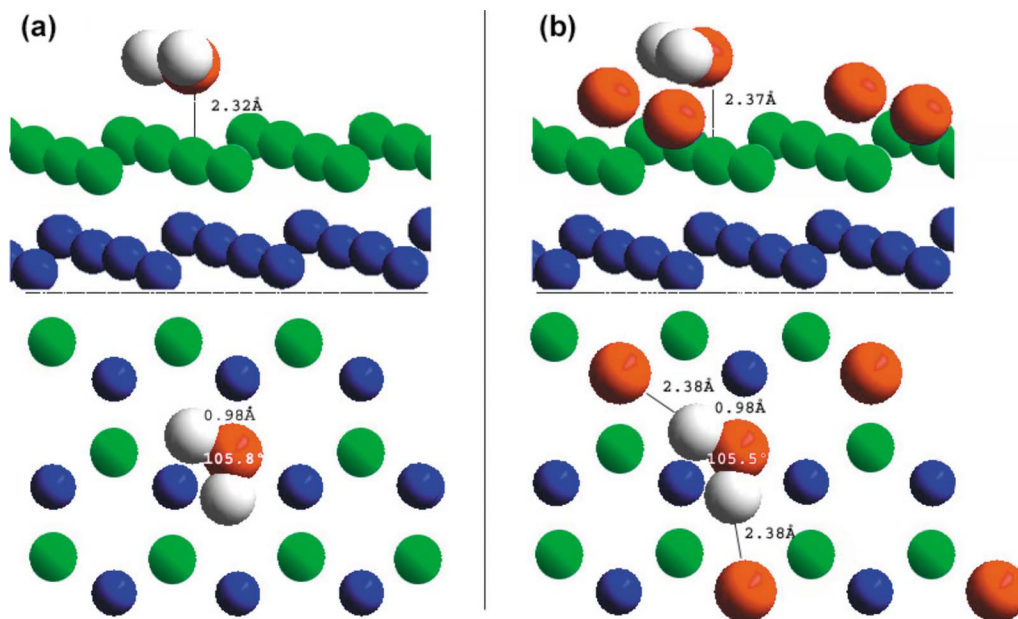


FIG. 2. (Color online) Adsorption geometries of water (a) on Ru(0001) and (b) on O(2×2)/Ru(0001). Green circles indicate Ru atoms in the topmost layer (top sites), and blue circles Ru atoms in the second layer (hcp sites). Red and white circles represent oxygen and hydrogen atoms, respectively. The same color code is kept in all the figures.

the substrate oxygens were also proposed by Doering and Madey for water deposition on O(2×2)/Ru(0001) surface.⁷ However, in that structure, the molecular plane is perpendicular to the surface. A molecule parallel to the substrate and hydrogen bonded with preadsorbed oxygen was proposed by Pache *et al.* for the adsorption of water on O(2×2)/Ni(111) surface,⁸ although a fcc site was assumed in that work.

We also checked that the preferred adsorption site and geometry does not change appreciably when increasing the lateral extension of the supercell. For example, for a water coverage of 0.0625 ML (see also Fig. 4 below), the molecules lie in the top-site and/or parallel configuration, although at a slightly lower height over the substrate (2.28 Å) and forming two extended hydrogen bonds of 2.42 Å. This coverage can be considered as representing an isolated monomer. Its calculated adsorption energy of 616 meV is just 26 meV higher than at 0.25 ML. As we will see below for an intermediate coverage of 0.125 ML, our calculated adsorption energy is 624 meV, i.e., almost identical to the 0.0625 ML case.

It is interesting to compare the characteristics of the water adsorption on the oxygen covered and clean Ru(0001) surfaces. We thus studied the adsorption of water on clean Ru(0001) at 0.25 ML coverage using the same computational parameters as in the O(2×2)/Ru(0001) case. We found that the molecule also sits on a Ru-top position, 2.32 Å above the substrate, with the molecular plane almost parallel to the surface, with an adsorption energy $E_{ads}=370$ meV, in good agreement with previously reported values.^{1,11,24} An illustration of the optimized adsorption geometries of water on clean Ru(0001) and on O(2×2)/Ru(0001) is shown in Fig. 2. In both cases, the molecule sits approximately at the same distance from the substrate Ru atoms and keeps the same values of OH bond length and bond angle.

The different adsorption energies in clean Ru(0001) and O(2×2)/Ru(0001) surfaces can be attributed to the hydrogen bonding with the chemisorbed oxygen atoms in the O(2×2)/Ru(0001) surface, with each bond contributing 110 meV to the adsorption energy. Formation of hydrogen bonds between water molecules and preadsorbed oxygen has also been proposed for water deposition on O(1×1)/Ru(0001) surface.¹¹ It is interesting to note that, although the hydrogen bond length with the chemisorbed O of the O(2×2)/Ru(0001) is significantly longer than in other hydrogen bonded systems, the energy gain associated with the hydrogen bonding is similar. This is probably an indication of the strong polarization of the chemisorbed oxygen atoms in the O(2×2)/Ru(0001) surface.

The considerable increase in adsorption energy on the O(2×2) surface with respect to clean Ru could explain the larger stability of water against dissociation in the former case.¹² In addition to increasing the binding energy, the chemisorbed O atoms in the O(2×2)/Ru(0001) provide a preferential orientation to the adsorbed water molecules which is absent in the case of clean Ru(0001).

B. Comparison with experimental scanning tunneling microscope images

To determine the adsorption sites of water in the experimental STM images, the different high symmetry sites in the surface need to be identified, which is usually not a trivial task. Fortunately, in the O(2×2)/Ru(0001) superstructure, this can be done by studying the dependence of the STM images on the tunneling parameters, as shown in previous work.^{19,20} The calculated images in Fig. 3 show the change of relative contrast between top and fcc sites for different bias polarities. For positive sample bias, the top sites appear

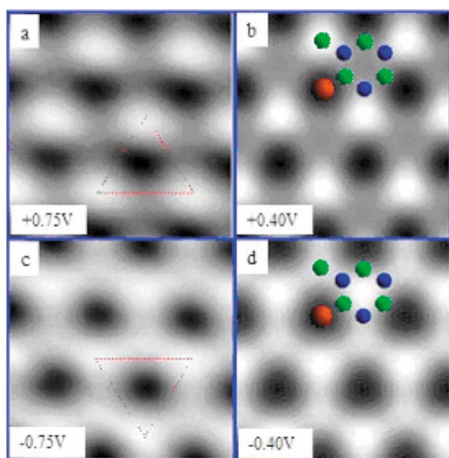


FIG. 3. (Color online) [(a) and (c)] Experimental and [(b) and (d)] theoretical STM images of $O(2 \times 2)/Ru(0001)$ before water adsorption showing different contrasts at different bias polarities: ± 0.75 V for experiment and ± 0.40 V for the simulation. In panels (b) and (d), the positions of the Ru atoms in the topmost (green) and second (blue) layers are schematically indicated. The red dot corresponds to the chemisorbed hcp oxygen atom. Notice that, at positive bias, top Ru sites appear brighter, whereas at high enough negative bias, the brightest spots correspond to the fcc sites. This contrast reversal makes the identification of the different adsorption sites using STM possible. The difference between fcc and top sites is larger at positive polarities, both in the (a) experimental and (b) simulated STM images.

brighter than fcc sites, but for negative bias voltage, the contrast is reversed. The experimental images agree very well with this bias dependent contrast behavior, providing a complete determination of the adsorption site.

Panel (a) in Fig. 4 shows an experimental STM image for water adsorbed at low coverage on $O(2 \times 2)/Ru(0001)$, with a simulated image of water in a 4×4 supercell (corresponding to a coverage of 0.0625 ML) in panel (b). Water molecules appear as bright protrusions. The registry of the ad-

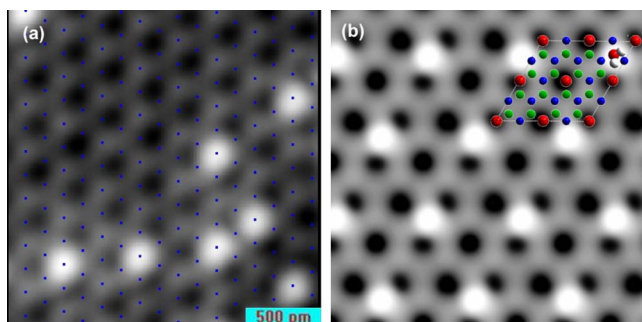


FIG. 4. (Color online) (a) Experimental STM image at a constant current of 100 pA and an applied voltage of 200 meV. Brightest dots correspond to adsorbed water molecules, and the weaker spots to the topmost Ru atoms in the $O(2 \times 2)/Ru(0001)$ substrate. A lattice of blue dots has been superimposed to mark the positions of the Ru atoms in the first layer. (b) Simulated STM image for 0.0625 ML of water adsorbed with 4×4 periodicity on the $O(2 \times 2)/Ru(0001)$ surface at constant current; the bias voltage is 400 meV.

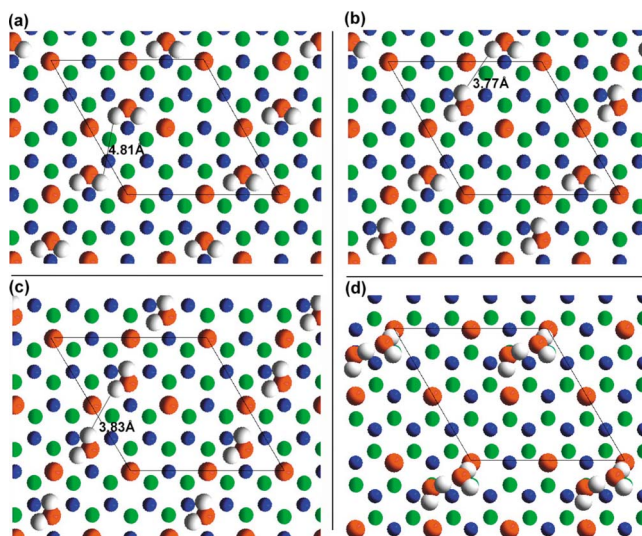


FIG. 5. (Color online) Different water configurations at 0.125 ML coverage after relaxation. Structures (a)–(c) are formed by parallel rows of water monomers with different orientations relative to each other and with respect to the direction of the row. In these configurations, water molecules adsorb 2.28 – 2.29 Å above a Ru atom in topmost layer and form long (2.37 – 2.54 Å) hydrogen bonds with oxygen atoms in the substrate. Structure in panel (d) is formed by water dimers. One of the molecules in the dimer has its oxygen placed at 2.22 Å over a top Ru site and is hydrogen bonded to a surface oxygen atom (2.22 Å O-H bond length) and to the adjacent molecule (1.62 Å). The adjoining molecule keeps its oxygen atom 3.63 Å above the Ru topmost layer, and it is also hydrogen bonded to the oxygen atom below (1.76 Å).

sorbed water molecules with the substrate was determined from the previously identified sites in the STM images, as described above. The blue dots in panel (a) of Fig. 4 highlight all the Ru top sites in the surface. The bright spots far from the water molecules can be unambiguously identified as the Ru top sites exposed inside the $O(2 \times 2)$ unit cell. One can see that, at least at low temperatures, the water molecules always sit on those Ru-top sites.

C. Interaction between water molecules

To check the effect of different arrangements of neighboring molecules in the energetics of the adsorption, we increased the water coverage to 0.125 ML by placing a second monomer in the 4×4 supercell. Our simulations indicate that both molecules relax to similar top-site and/or parallel adsorption geometries. Four nonequivalent configurations were obtained depending on the relative orientation of the two monomers in the cell. Panels (a)–(c) in Fig. 5 show the most stable of those arrangements. In these configurations, the molecules lay 2.28 Å over top Ru sites, keeping their “extended” hydrogen bonds with the oxygen atoms underneath (oxygen atoms chemisorbed to the substrate) in the range of 2.35 – 2.50 Å. Thus, we can conclude that the energy differences between different configurations are due to the interaction between neighboring molecules. Configuration (a) corresponds to the optimum relative orientation of nearest-

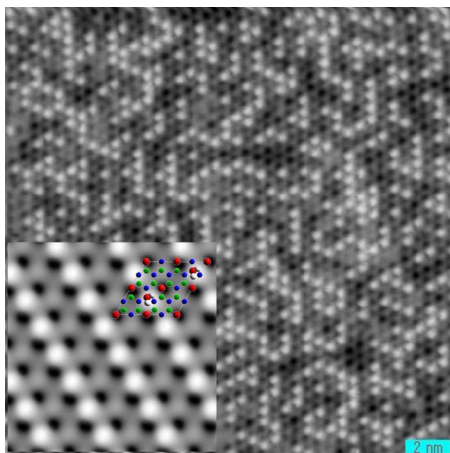


FIG. 6. (Color online) Experimental STM image taken at 6 K at a constant current of 47 pA and an applied bias voltage of 70 mV. The sample was previously annealed to 140 K. Inset (lower left): Simulated STM image for configuration (a) of Fig. 5, corresponding to 0.125 ML of water adsorbed on the $O(2 \times 2)/\text{Ru}(0001)$ surface for an applied voltage of +150 meV (image scale is larger than the experimental one). A schematic diagram of the adsorption geometry is also included.

neighbor molecular dipoles, with 624 meV per molecule. Configuration (b) is 25 meV less stable, and configuration (c) is the least stable one, with 584 meV per molecule.

We can correlate the stability of the different configurations with the repulsion between hydrogen atoms in neighboring water molecules. In case (a), the closest distance between the hydrogen atoms is 4.81 Å, whereas this separation is reduced to 3.77 and 3.83 Å in configurations (b) and (c), respectively (see Fig. 5). Two water molecules are bound to the same oxygen atom in configurations (b) and (c) [one shared oxygen in (b) and two in (c)], resulting in a smaller H-H distance. Besides this purely geometric effect, the “sharing” of oxygen atoms can also affect the stability of the long water-oxygen hydrogen bonds. This could cause a further reduction of the adsorption energy in these configurations.

Figure 6 displays an experimental STM image that shows a tendency of the adsorbed water molecules to form short linear row structures at intermediate coverage, rather than denser two-dimensional patches. This is consistent with our observation that at 0.25 ML coverage, the adsorption energy of water is lower than in more dilute layers. The calculated energy difference between structures at 0.125 and 0.0625 ML also indicates a small attractive interaction, ~ 8 meV, between neighboring molecules. It is not clear, however, that this is strong enough to be responsible for the formation of rows. The inset of Fig. 6 shows the simulated STM image for configuration (a) of Fig. 5. It is hardly distinguishable from the simulated STM images corresponding to configurations (b) and (c). This illustrates the difficulty of obtaining detailed information about the relative orientation of the molecules in the experimental images.

D. Formation of dimers

We have also studied a fourth configuration at 0.125 ML coverage. It is displayed in panel (d) in Fig. 5. In this struc-

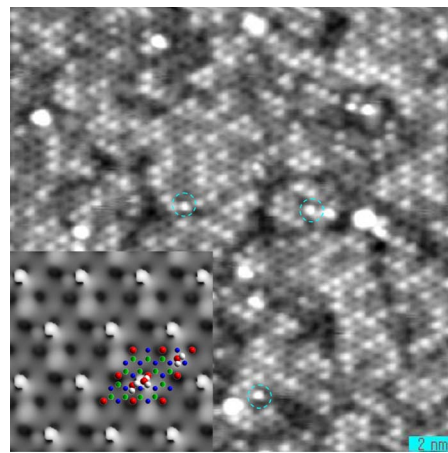


FIG. 7. (Color online) Experimental STM image taken at 6 K at a constant current of 100 pA and an applied voltage of 100 mV. The sample had been previously annealed to 180 K. The dashed blue circles enclose brighter spots that are tentatively assigned to dimers, by comparison with theoretical STM images, like the one shown in the inset. The inset displays a constant current simulated STM image for one dimer and one monomer adsorbed on a 2×2 unit cell of the $O(2 \times 2)/\text{Ru}(0001)$ surface for an applied voltage of +150 meV. The dimer is much brighter than the monomer.

ture, pairs of water molecules form a hydrogen bonded water dimer on the surface. Configurations (a) and (d) of Fig. 5 are energetically almost degenerate with an adsorption energy of 624 meV per water molecule. The calculated adsorption energy of the adsorbed dimer relative to the freestanding one is 1.01 eV (505 meV per molecule). The difference between these two values, 238 or 119 meV per water molecule, gives the binding energy due to the hydrogen bond within the water dimer. We have also checked the stability of this structure against desorption of one of the molecules forming the dimer. The energy cost to desorb the highest molecule is 632 meV, showing clearly that both molecules have quite similar binding energies in this configuration. Thus, coexistence of water dimers and monomers on the $O(2 \times 2)/\text{Ru}(0001)$ surface is plausible due to the almost degenerate adsorption energies. The inset of Fig. 7 shows a simulated STM image for a system in which a water monomer and dimer are coadsorbed on the same 4×4 unit cell. The dimers appear as brighter protrusions than the monomers, which reflect the topography of the system: One of the molecules forming the dimer sits 3.63 Å above the substrate, while the height of the adsorbed water monomer is just 2.28 Å. Many experimental STM images (see Fig. 7) show bright spots that could be assigned to dimers according to the theoretical calculations. Unfortunately, besides the topographic contrast, there is not sufficiently strong experimental evidence at the moment to confirm the assignment. An important observation in connection to these brighter spots is that they were only seen after annealing the sample to approximately 180 K, which is close to the desorption temperature. This could indicate that the formation of dimers requires overcoming relatively large energetic barriers. One could also assign the bright dots to water monomers that are adsorbed in configurations different from the most stable top-site

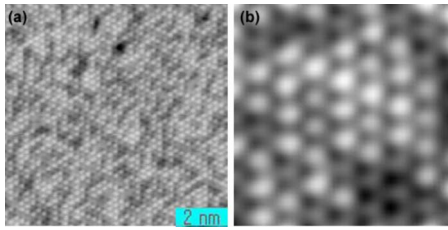


FIG. 8. (Color online) Experimental STM images of a $O(2 \times 2)$ -Ru(0001) surface with a water coverage of 0.18 ML, close to the saturation of the $p(2 \times 2)$ phase, acquired at 6 K. (a) Large scan area ($20 \times 20 \text{ nm}^2$) showing (2×2) patches of water, acquired at constant current of 95 pA and an applied bias voltage of -220 mV after annealing to 140 K. (b) Enlarged view ($3 \times 3 \text{ nm}^2$) of a local $p(2 \times 2)$ structure of water molecules taken at 83 pA and 50 mV.

and/or parallel geometry. This, however, seems quite improbable for two reasons: (i) The only alternative geometry found in our calculations has an almost negligible adsorption energy and (ii) when the substrate is imaged after dosing at low temperature ($\sim 25 \text{ K}$), no bright dots are seen and fuzzy lines, most probably due to unstable molecules being dragged by the tip, appeared instead.

Increasing the water coverage leads to the formation of (2×2) patches of water as the coverage approaches 0.25 ML, as shown in Fig. 8. This structure is observed to be stable at temperatures up to 180 K.

E. Higher water coverage

We have also explored theoretically the possible existence of other structures corresponding to higher water coverage. For example, we have placed a second water molecule on the same 2×2 unit cell, corresponding to 0.5 ML. In this structure, no Ru-top sites are available for adsorption of the second molecule. Therefore, it cannot adopt the characteristic top-site and/or parallel structure of the monomers at low coverage. We found that the second water molecule prefers to form a hydrogen bond with the preadsorbed molecule rather than to bind to Ru hcp or fcc sites. The water molecules at 0.5 ML therefore adopt a dimer configuration whose optimized geometry is shown in Fig. 9(a), along with the corresponding simulated STM image on panel (b). The second water molecule sits at 3.61 \AA , forming one hydrogen bond of 2.12 \AA with the oxygen atom underneath and another hydrogen bond of 1.67 \AA with the first monomer. Furthermore, the preadsorbed monomer also varies its orientation, tilting its atomic plane slightly in order to optimize the hydrogen bond, with an O-H distance of 1.73 \AA to one of the surface oxygen atoms. The adsorption energy (per water molecule) for this relaxed configuration is 599 meV , comparable to the 590 meV value found for the monomers at 0.25 ML.

Experimentally the highest coverage investigated was slightly above 0.25 ML. The STM images are composed by fuzzy lines superimposed on the stable (2×2) water pattern on the $O(2 \times 2)$ overlayer. These lines are due to the tip dragging molecules on the surface. The lack of observed ordered structures above 0.25 ML seems to indicate that a

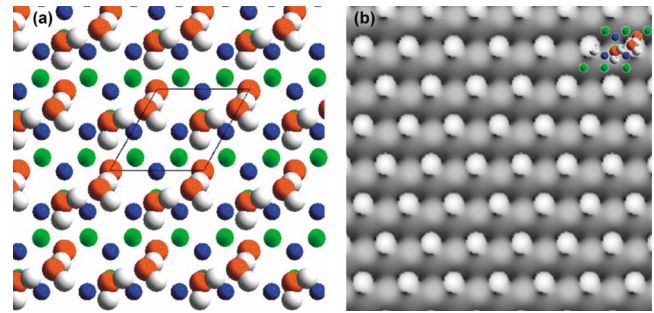


FIG. 9. (Color online) (a) Calculated water configuration at 0.5 ML coverage. The structure is formed by dimers in which one of the molecules has its oxygen 2.26 \AA above a Ru-top site and it is hydrogen bonded to one of the surface oxygen atoms (2.12 \AA O-H bond length) and to the adjacent water molecule (1.67 \AA). The second molecule adsorbs 3.61 \AA above the Ru topmost layer, and it is hydrogen bonded to the substrate oxygen atom right below (1.73 \AA). (b) Simulated STM image of the corresponding configuration. Applied voltage: $+150 \text{ meV}$. A schematic diagram of the adsorption geometry is also included.

large energy barrier needs to be overcome in order to generate structures such as that depicted in Fig. 9(a).

V. CONCLUSIONS

Density functional calculations show that water monomers preferentially sit on the Ru-top sites in the unit cell of the $O(2 \times 2)$ /Ru(0001) surface. This adsorption site has been experimentally confirmed using the distinct and characteristic voltage dependence of the STM images on $O(2 \times 2)$ /Ru(0001). The water molecular dipole is oriented almost parallel to the surface and the H atoms point toward the surface O atoms forming extended hydrogen bonds. The additional hydrogen bonding increases the adsorption energy with respect to that on clean Ru(0001) surface. The calculated adsorption energy per water molecule is in the range $590\text{--}624 \text{ meV}$, with a weak dependence on coverage from 0.0625 to 0.5 ML. In both experimental and calculated STM images, the water molecules are imaged as protrusions. At water coverage below 0.25 ML, a tendency to form rows is experimentally observed. Theoretically, the interaction energy between neighbor water molecules, as deduced from the variation of the adsorption energy with coverage, is small. However, it is interesting to note that the highest adsorption energy found in our calculations corresponds to 0.125 ML coverage [configuration (a) in Fig. 5]. This optimal structure consists of parallel rows of water monomers with preferred relative orientation and with a separation between rows of 4.7 \AA . Our calculations also show that water dimers have a similar stability as the monomers. The dimers appear as noticeably brighter dots in the simulated STM images. Although pronounced dots can also be found in many experimental images, the evidence for the existence of such dimers in the surface under the present experimental conditions is not firm enough and needs further investigation. It has to be noted, in particular, that the bright dots only appear in samples that have been annealed at temperatures close to the

desorption temperature. In general, as the coverage increases, we can expect a large number structure with similar energies, as happens in other water covered surfaces.²⁵ Molecular dynamic simulations at finite temperature would help understand this regime.

ACKNOWLEDGMENTS

This work has been supported by the Basque Departamento de Educación, the UPV/EHU (Grant No. 9/UPV 00206.215-13639/2001), the Spanish Ministerio de Educación y Ciencia (Grant No. FIS2004-06490-C3-00), the Eu-

ropean Network of Excellence FP6-NoE NANOQUANTA (Grant No. 500198-2), and the projects NANOMATERIALES and NANOTRON funded by the Basque Departamento de Industria, Comercio y Turismo within the ETORTEK program, and the Departamento para la Innovación y la Sociedad del Conocimiento from the Diputación Foral de Guipúzcoa. The experimental work was supported by the Director, Office of Energy Research, Office of Basic Energy Sciences, Materials Sciences Division, of the U.S. Department of Energy under Contract No. DE-AC02-05CH11231. A.M. was financed by the Marie Curie Outgoing International Foundation, Project No. 514412.

-
- ¹A. Michaelides, V. A. Ranea, P. L. de Andres, and D. A. King, *Phys. Rev. Lett.* **90**, 216102 (2003).
²T. Mitsui, M. K. Rose, E. Fomin, D. F. Ogletree, and M. Salmeron, *Science* **297**, 1850 (2002).
³J. Cerdá, A. Michaelides, M. L. Bocquet, P. J. Feibelman, T. Mitsui, M. Rose, E. Fomin, and M. Salmeron, *Phys. Rev. Lett.* **93**, 116101 (2004).
⁴G. Held and D. Menzel, *Surf. Sci.* **327**, 301 (1995).
⁵C. Nobl, C. Benndorf, and T. E. Madey, *Surf. Sci.* **157**, 29 (1985).
⁶F. Traeger, D. Langenberg, Y. K. Gao, and C. Wöll, *Phys. Rev. B* **76**, 033410 (2007).
⁷D. L. Doering and T. E. Madey, *Surf. Sci.* **123**, 305 (1982).
⁸T. Pache, H. P. Steinruck, W. Huber, and D. Menzel, *Surf. Sci.* **224**, 195 (1989).
⁹K. D. Gibson, M. Viste, and S. J. Sibener, *J. Chem. Phys.* **112**, 9582 (2000).
¹⁰M. Nakamura and M. Ito, *Phys. Rev. Lett.* **94**, 035501 (2005).
¹¹M. M. Thiam, T. Kondo, N. Horimoto, H. S. Kato, and M. Kawai, *J. Phys. Chem. B* **109**, 16024 (2005).
¹²M. J. Gladys, A. Mikkelsen, J. N. Andersen, and G. Held, *Chem. Phys. Lett.* **414**, 311 (2005).
¹³G. Kresse and J. Hafner, *Phys. Rev. B* **47**, 558 (1993).
¹⁴G. Kresse and J. Hafner, *Phys. Rev. B* **49**, 14251 (1994).
¹⁵G. Kresse and J. Furthmüller, *Phys. Rev. B* **54**, 11169 (1996).
¹⁶J. P. Perdew, J. A. Chevary, S. H. Vosko, K. A. Jackson, M. R. Pederson, D. J. Singh, and C. Fiolhais, *Phys. Rev. B* **46**, 6671 (1992).
¹⁷P. E. Blochl, *Phys. Rev. B* **50**, 17953 (1994).
¹⁸G. Kresse and D. Joubert, *Phys. Rev. B* **59**, 1758 (1999).
¹⁹F. Calleja, A. Arnau, J. J. Hinarejos, A. L. V. de Parga, W. A. Hofer, P. M. Echenique, and R. Miranda, *Phys. Rev. Lett.* **92**, 206101 (2004).
²⁰C. Corriol, F. Calleja, A. Arnau, J. J. Hinarejos, A. L. V. de Parga, W. A. Hofer, and R. Miranda, *Chem. Phys. Lett.* **405**, 131 (2005).
²¹J. Tersoff and D. R. Hamann, *Phys. Rev. Lett.* **50**, 1998 (1983).
²²J. Tersoff and D. R. Hamann, *Phys. Rev. B* **31**, 805 (1985).
²³T. K. Shimizu, A. Mugarza, J. I. Cerdá, M. Heyde, Y. Qi, U. D. Schwarz, D. F. Ogletree, and M. Salmeron (unpublished).
²⁴A. Michaelides, A. Alavi, and D. A. King, *J. Am. Chem. Soc.* **125**, 2746 (2003).
²⁵P. Cabrera-Sanfeliix, A. Arnau, G. R. Darling, and D. Sanchez-Portal, *J. Chem. Phys.* **126**, 214707 (2007).